

# Non-proliferative effects of lysophosphatidic acid enhance cortical growth and folding

Marcy A Kingsbury<sup>1,2,4</sup>, Stevens K Rehen<sup>1,2,4</sup>, James J A Contos<sup>2</sup>, Christine M Higgins<sup>1,3</sup> & Jerold Chun<sup>1,2</sup>

Lysophosphatidic acid (LPA) is a phospholipid that has extracellular signaling properties mediated by G protein-coupled receptors. Two LPA receptors, LPA<sub>1</sub> and LPA<sub>2</sub>, are expressed in the embryonic cerebral cortex, suggesting roles for LPA signaling in cortical formation. Here we report that intact cerebral cortices exposed to extracellular LPA *ex vivo* rapidly increased in width and produced folds resembling gyri, which are not normally present in mouse brains and are absent in LPA<sub>1</sub> LPA<sub>2</sub> double-null mice. Mechanistically, growth was not due to increased proliferation but rather to receptor-dependent reduced cell death and increased terminal mitosis of neural progenitor cells (NPCs). Our results implicate extracellular lipid signals as new influences on brain formation during embryonic development.

The remarkable increase in cerebral cortical size across mammalian evolution is characterized by increased cell number leading to the expansion of cortical surface area<sup>1</sup>. In larger mammalian brains, this expansion often produces folds that form sulci and gyri. Changes in the regulation of neural cell death, proliferation and differentiation within the embryonic neuroepithelium overlying the lateral ventricles, termed the ventricular zone (VZ), are thought to cause these pronounced changes in cortical size<sup>2–4</sup>. A variety of extracellular factors have been shown to influence NPCs and young neurons of the cortex. Neurotransmitters<sup>5</sup> and peptide factors<sup>6–8</sup> affect neurogenic parameters of developing cortical cells, although it is generally unclear how these signals influence the growth and morphology of the intact cerebral cortex. Two possible exceptions are fibroblast growth factor 2 (FGF2) and pituitary adenylate cyclase-activating polypeptide, which increase and decrease the proliferative pool, respectively, when administered intraventricularly<sup>9,10</sup>.

A candidate lipid molecule for regulating neurogenic processes, and hence cortical size, is LPA. Many of LPA's effects are mediated by G protein-coupled receptors that are members of the lysophospholipid receptor gene family<sup>11,12</sup>. Two receptors, LPA<sub>1</sub> and LPA<sub>2</sub>, show enriched gene expression in the mouse embryonic cortex<sup>13–15</sup>. Furthermore, LPA signaling stimulates cytoskeletal reorganization, cell rounding and depolarizing ionic conductances in wild-type NPCs from the VZ<sup>16,17</sup> and has modest proliferative effects on NPCs in culture<sup>18</sup>. However, LPA<sub>1</sub>-null and LPA<sub>1</sub> LPA<sub>2</sub> double-null mice reaching adulthood do not show obvious defects in cortical organization, although they do exhibit 50% perinatal lethality, olfactory defects and occasional reductions in cortical width<sup>18,19</sup>.

Complementing receptor loss-of-function studies, LPA receptor gain-of-function can be accomplished by increasing receptor activation through exogenous delivery of LPA. We therefore developed an

*ex vivo* cortical culture system in which LPA exposure of intact brain could be regulated. Our results show that LPA exposure rapidly induces folding and widening of the cerebral wall. The observed cortical growth was absent from LPA<sub>1</sub> LPA<sub>2</sub> double-null mice and is attributable to increased terminal mitosis and decreased cell death within the VZ.

## RESULTS

### *Ex vivo* system simulates *in vivo* environment

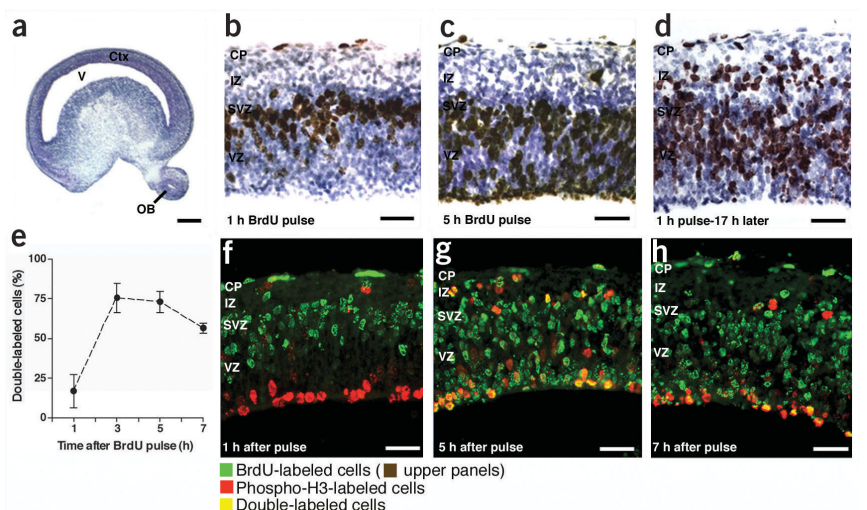
Under standard conditions, cultured hemispheres resembled cortices *in vivo*, maintaining their normal morphology and neurogenic gradients (Fig. 1a). As NPCs within the cerebral cortical VZ progress through the cell cycle, they translocate their nuclei from the top to the bottom of the VZ by a process called interkinetic nuclear migration<sup>20,21</sup>. After each mitosis (M-phase) at the bottom of the VZ, a fraction of daughter cells known as 'early postmitotic neurons' exits the cell cycle while a complementary fraction maintains the proliferative pool by undergoing a new round of DNA synthesis (S-phase) at the top of the VZ<sup>2</sup>. Examination of proliferating NPCs using bromodeoxyuridine (BrdU) pulses showed that the position of S-phase cells and interkinetic nuclear migration were preserved in the *ex vivo* cultures (Fig. 1b,c). Labeling for M-phase cells using an antibody specific to the phosphorylated form of histone H3 (anti-phospho-H3)<sup>22</sup> showed that dividing cells were located at the bottom of the VZ in control explants (see Fig. 5b), as observed *in vivo*<sup>23</sup>. In addition, cell migration into the intermediate zone (IZ; Fig. 1d) and cortical growth (data not shown) were maintained during culture. Finally, cell cycle parameters *ex vivo* were indistinguishable from those reported *in vivo*. For analysis of cell cycle progression, S-phase cells labeled by a 1-h BrdU pulse were examined at subsequent time points for entry and exit from M-phase using immunolabeling for anti-phospho-H3.

<sup>1</sup>Department of Molecular Biology, The Scripps Research Institute, 10550 North Torrey Pines Road, ICND 118, La Jolla, California 92037, USA. <sup>2</sup>Department of Pharmacology, The University of California at San Diego, 9500 Gilman Drive, La Jolla, California 92093, USA. <sup>3</sup>Neuroscience Program, The University of California at San Diego, 9500 Gilman Drive, La Jolla, California 92093, USA. <sup>4</sup>These authors contributed equally to this work. Correspondence should be addressed to J.C. (jchun@scripps.edu).

**Figure 1** *Ex vivo* culture system simulates *in vivo* neurogenic parameters. (a) Cresyl violet–stained sagittal section from an E14 cortical hemisphere cultured for 17 h in control medium. Ctx, cortex; OB, olfactory bulb; V, ventricle. Scale bar, 250  $\mu$ m.

(b) Cresyl violet–stained cross-section through a control hemisphere showing the location of labeled S-phase cells (brown) following a 1-h BrdU pulse. CP, cortical plate; IZ, intermediate zone; SVZ, subventricular zone; VZ, ventricular zone. (c) Cross-section showing the migration of labeled S-phase cells to the bottom of the VZ following a 5-h BrdU pulse. (d) Cross-section showing that cells initially labeled in S-phase have migrated into the IZ 17 h after a BrdU pulse. (e–h) Cell cycle phase transition *ex vivo* is similar to *in vivo*. (e) After 10 h *ex vivo*, a 1-h BrdU pulse was given to track the progression of labeled S-phase cells through mitosis. The number of cells double-

labeled with anti-BrdU and anti-phospho-H3 (an M-phase marker) was counted at 1, 3, 5 and 7 h after the pulse and expressed as a percentage of the total number of mitotic cells. (f–h) Cross-sections immunolabeled with anti-BrdU (green) and anti-phospho-H3 (red) from control hemispheres showing the location of labeled S-phase and M-phase cells, respectively. Cortices showed very few double-labeled cells (yellow) at 1 h (f), many at 5 h (g) and a decreased percentage at 7 h (h). Scale bars in b–d and f–h, 50  $\mu$ m.



Whereas very few S-phase cells (BrdU-labeled cells) had entered mitosis (*i.e.*, double-labeled with anti-phospho-H3) 1 h after the pulse (Fig. 1e,f), a maximum number had entered mitosis at 3 h (Fig. 1e), consistent with reports *in vivo*<sup>24</sup>. The number of labeled S-phase cells in mitosis remained high at 5 h (Fig. 1e,g) but decreased by 7 h (Fig. 1e,h), indicating that progression through S, G2 and M phases *ex vivo* is in agreement with the estimated combined duration (5.8–8.6 h) for S, G2 and M phases *in vivo*<sup>24–26</sup>. Collectively, these results indicate that, over the period examined, the *ex vivo* culture system mimics cerebral cortical development *in vivo*.

### LPA induces folding and widening of the cerebral wall

To examine the effects of exogenous LPA exposure, the two cerebral hemispheres from single animals were physically separated so that one could be cultured with LPA (1  $\mu$ M) while the other was cultured in control medium (Fig. 2a). Embryonic day 14 (E14) cortices were used, as LPA<sub>1</sub> and LPA<sub>2</sub> gene expression is high at this age<sup>13,14</sup>, and E14 is the midpoint of mouse cortical neurogenesis. Hemispheres exposed to LPA for 17 h *ex vivo* showed striking cortical folding as compared to opposite hemispheres obtained from the same animals (Fig. 2b,c). These folds were also visible to the unaided eye before sectioning (Fig. 2d,e). A time course analysis

revealed a maximum percentage of folded cortices at 16 h (Fig. 3a). Within an individual hemisphere, folding was evident only at later time points and became more pronounced with increased time *ex vivo* (Fig. 3b). Cortical folding further increased when culture time was extended from 16 h to 24 h *ex vivo* and did not show evidence of reversibility (data not shown).

An analysis of cross-sections through cortex showed that LPA-treated hemispheres were ~30% thicker than controls (Fig. 4a,b). Both postmitotic and proliferative regions were affected (IZ/cortical plate (CP) and VZ, respectively; Fig. 4c). Cell counts revealed a 34% and 22% increase in the VZ and IZ/CP, respectively, following LPA treatment (Fig. 4d). These cell counts were done by comparing matched sagittal cross-sections from anterior, middle and posterior cortex in control and LPA-treated hemispheres from the same animal. No change in cell density within the VZ ( $n = 7$  matched pairs,  $P = 0.95$ , paired *t*-test) or IZ/CP ( $n = 7$  matched pairs,  $P = 0.69$ , paired *t*-test) was observed. Average cell diameter (see Methods) was also not significantly changed following LPA treatment (control,  $6.6 \pm 1.3 \mu$ m; LPA,  $7.0 \pm 1.4 \mu$ m;  $n = 3$  matched pairs;  $P = 0.23$ , paired *t*-test), despite the occurrence of known morphological changes<sup>17</sup>. All together, these results show that LPA exposure can alter cortical folding, thickness and cell number without altering cell density.

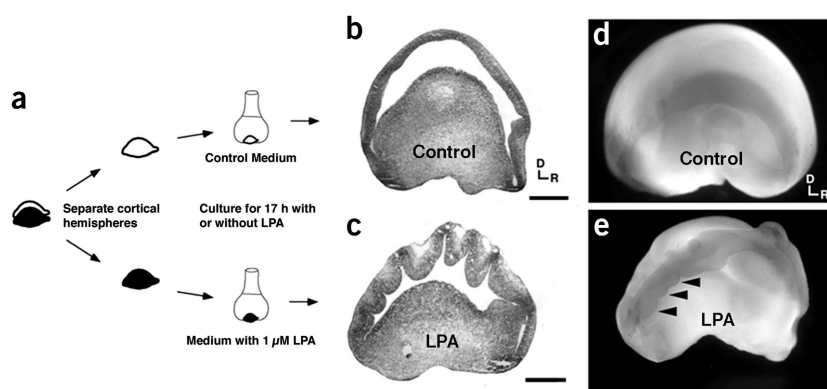


**Figure 2** LPA induces cortical folds.

(a) Flowchart summarizing protocol for *ex vivo* culture. (b,c) Cresyl violet–stained sagittal sections of E14 hemispheres from the same animal showing extensive cortical folding after culture with LPA (c) compared to control medium (b). D, dorsal; R, rostral. Scale bars, 0.5 mm. (d,e) Whole-mount views of hemispheres following 17 h culture in control medium (d) or medium with LPA (e). The LPA-treated cortex shows cortical folds (arrowheads) that extend throughout the cerebral hemisphere. Overall circumferential dimensions of the cortex did not significantly change after LPA treatment ( $n = 9$  matched pairs,  $P = 0.41$ , paired *t*-test).

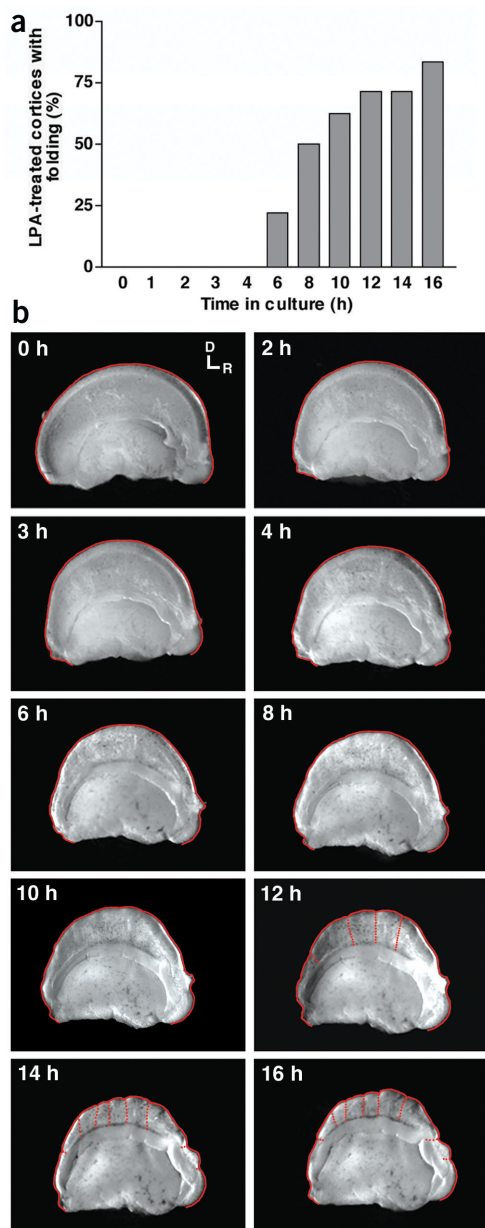


**Figure 3** Cortical folds arise at later time points in culture.

(a) Histogram showing percentage of LPA-treated hemispheres with cortical folds at successive time points *ex vivo*. (b) Real-time whole-mount views showing time course of folding *ex vivo* for a single LPA-treated hemisphere. Dotted red lines highlight the appearance of cortical folds. D, dorsal; R, rostral.

without a corresponding increase in S-phase cells suggests that LPA increases terminal mitosis of NPCs, promoting their cell cycle exit. If this were the case, LPA-treated cortices should have more postmitotic neurons than controls. Indeed, after LPA treatment, more cells were labeled with anti- $\beta$ -tubulin-III (Fig. 5e,f), a marker of early postmitotic neurons<sup>28</sup>. The observed increase of young neurons within the IZ/CP cannot be simply explained by faster migration, as LPA did not alter the number of BrdU-labeled cells migrating into the IZ after a short interval (Fig. 5g). These findings, combined with data showing that LPA simultaneously increases M-phase cells but not S-phase cells, suggest that LPA treatment promotes terminal mitosis of NPCs that then migrate out of the VZ, contributing to increased thickness of the postmitotic zone.

#### LPA decreases cell death in the VZ

An alternative and not mutually exclusive explanation for the increase in cortical growth after LPA exposure is decreased cell death. LPA has anti-apoptotic properties<sup>29</sup> that could affect programmed cell death in the embryonic VZ<sup>30,31</sup>. Apoptotic cells in tissue sections from cortical cultures were identified by two independent methods: *in situ* end-labeling plus (ISEL<sup>+</sup>)<sup>30</sup> and active caspase-3 immunofluorescence. Caspase-3-activated cell death is prominent in the VZ<sup>4</sup>. Compared to controls, LPA-treated cortices showed significantly fewer ISEL<sup>+</sup>-positive pyknotic nuclei (Fig. 6a–c). Immunolabeling for active caspase-3 yielded consistent results: cortices exposed to LPA had significantly fewer caspase-3-positive cells (Fig. 6d–f). These data indicate that LPA is a survival factor for cells within the embryonic cortical neuroepithelium.

#### LPA's effects are widespread and receptor-mediated

LPA's effects were observed throughout the cerebral cortex, both in rostral-caudal (Fig. 7) and lateral-medial dimensions (data not shown), consistent with the expression pattern of LPA receptor genes<sup>13–15</sup>. This does not rule out micro cortical domains, however, where differential effects could be observed. To determine whether LPA's effects in the *ex vivo* culture system are mediated by specific LPA receptors, we cultured, in the presence or absence of LPA, cortices from mice with null mutations in both LPA<sub>1</sub> and LPA<sub>2</sub>. Whereas LPA<sub>1</sub> is the likely candidate for mediating LPA's effects due to its restricted VZ expression<sup>14</sup>, LPA<sub>2</sub> is enriched in the embryonic postmitotic regions<sup>15</sup> and toward the end of neurogenesis<sup>13</sup>, suggesting its involvement in neuronal differentiation. Because both receptors can couple to the same G proteins and interchangeably mediate most effects of LPA in B103 neuroblastoma cells<sup>32</sup>, mice with null alleles of both receptors (double knockout) were examined to reduce possible compensation by either LPA receptor. LPA's effects on mitosis, cell death, cortical thickness and folding were not observed in cortices from double-null mutants. No statistically significant difference was observed in the number or distribution of phospho-H3-labeled cells in control versus LPA-treated cortices (Fig. 8a–c). Furthermore, double-null cortices treated with LPA did not show a reduction in active caspase-3 labeling (Fig. 8d–f). Together, these findings indicate that the LPA effects observed here are receptor-mediated.

#### LPA promotes terminal mitosis of NPCs

LPA is a well-known proliferative factor for several cell types<sup>27</sup>. To determine whether increases in cortical thickness and cell number following LPA exposure were due to increased proliferation, we used [<sup>3</sup>H]thymidine to measure DNA synthesis (S-phase). A 23% decrease in [<sup>3</sup>H]thymidine incorporation was observed in LPA-treated cortices relative to controls (Fig. 5a). However, when phospho-H3 immunolabeling was used to measure the number of NPCs in mitosis (M-phase), a 63% increase was observed following LPA treatment, as compared to controls (Fig. 5b–d). LPA also altered the location of mitotic cells, with LPA-treated cortices containing more phospho-H3-labeled cells at the top and middle of the VZ, as compared to controls ( $P = 0.03$  and  $P = 0.004$ , respectively; Fig. 5b,c). Despite their unusual location and increased number, dividing cells in LPA cortices were not arrested in mitosis (data not shown). These results show that LPA increases the number of cells in M-phase without increasing proliferation *per se*. The increase in mitotic figures

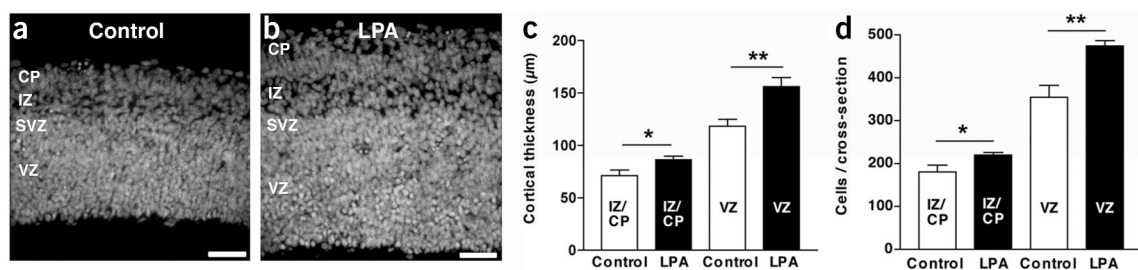


**Figure 4** LPA increases cortical thickness and cell number. (a,b) DAPI-labeled E14 cortices from the same animal showing increased cortical thickness following culture with LPA (b) compared to control medium (a). CP, cortical plate; IZ, intermediate zone; SVZ, subventricular zone; VZ, ventricular zone. Scale bars, 50  $\mu$ m. (c) Thickness of IZ/CP (postmitotic zone) and VZ from E14 control and LPA-treated hemispheres cultured for 17 h ( $n = 8$  matched pairs,  $*P = 0.02$ ,  $**P = 0.0004$ , paired  $t$ -tests). (d) Cell number in IZ/CP and VZ from matched cross-sections of E14 control and LPA-treated hemispheres cultured for 17 h ( $n = 7$  matched pairs,  $*P = 0.03$ ,  $**P = 0.003$ , paired  $t$ -tests).

## DISCUSSION

The major finding of the present study is that LPA signaling can alter cerebral cortical growth and anatomy. Exposing hemispheres to exogenous LPA produced cortical folds as well as rapid increases in thickness and cell number within both proliferative and postmitotic regions of cortex. The lack of LPA responses in cortices from LPA<sub>1</sub> LPA<sub>2</sub> double-null mice indicated that the effects were receptor-mediated.

While our data complement previous analyses of cortical growth, they also show marked differences. Disruption of cell death by deletion of the gene encoding caspase-3 or caspase-9 results in reduced NPC death and increased VZ size without a marked increase in CP thickness<sup>3,4,33</sup>. Augmented cell cycle re-entry by overexpression of  $\beta$ -catenin produces folds via the tangential expansion of cortical surface area without increases in cortical width<sup>34</sup>. By comparison, receptor-mediated

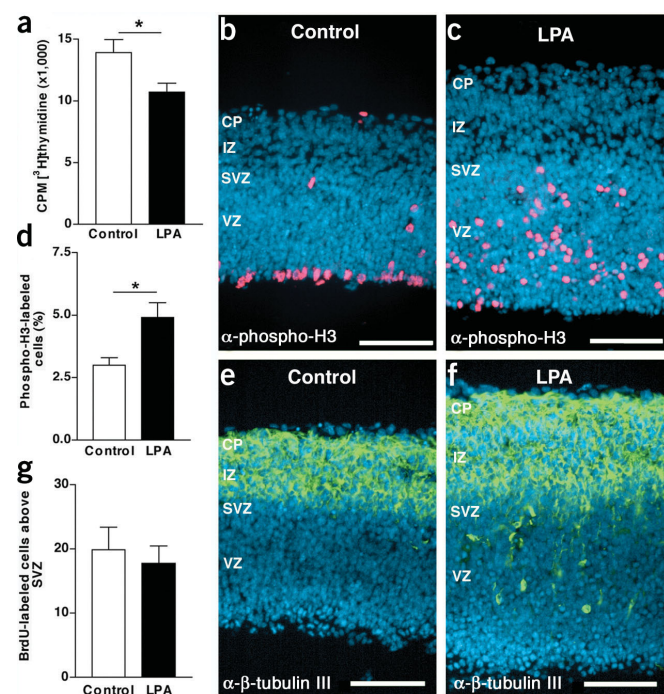


**Figure 5** LPA promotes terminal mitosis, but not faster migration, of NPCs. (a) Quantitation of DNA synthesis using [<sup>3</sup>H]thymidine incorporation (17 h exposure) following LPA-treatment compared to control ( $n = 12$  matched pairs,  $*P = 0.02$ , paired  $t$ -test). (b,c) DAPI-stained E14 cortices immunolabeled with anti-phospho-H3 (red), following culture with LPA (c) or control medium (b). CP, cortical plate; IZ, intermediate zone; SVZ, subventricular zone; VZ, ventricular zone. (d) Percentage of phospho-H3-labeled cells in cross-sections from control and LPA-treated cortices ( $n = 7$  matched pairs,  $*P = 0.03$ , paired  $t$ -test). (e,f) DAPI-stained E14 cortices immunolabeled for anti- $\beta$ -tubulin III (green) following culture with LPA (f) or control medium (e). (g) The number of BrdU-labeled cells above the SVZ in control and LPA-treated cortices 7 h after a short BrdU pulse ( $n = 4$  matched pairs,  $P = 0.74$ , paired  $t$ -test; see Methods for details). Scale bars (b,c,e,f) represent 100  $\mu$ m.

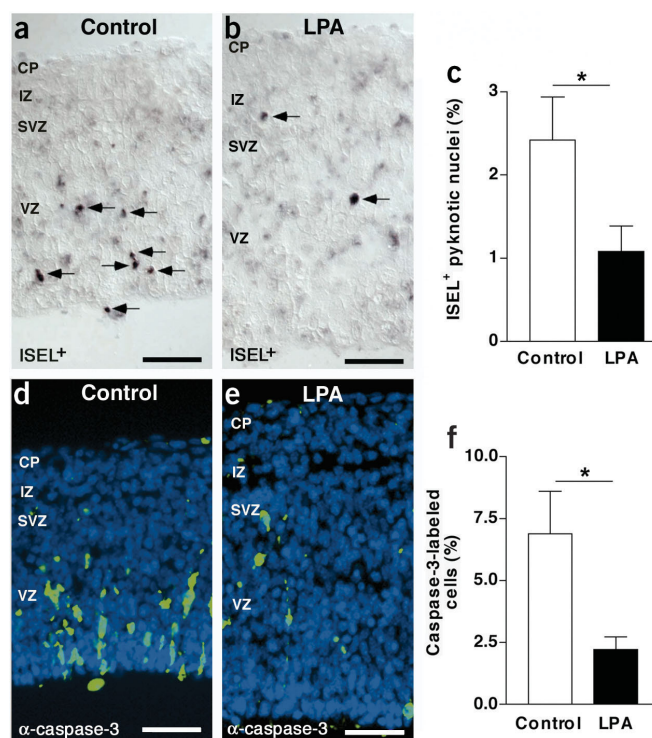
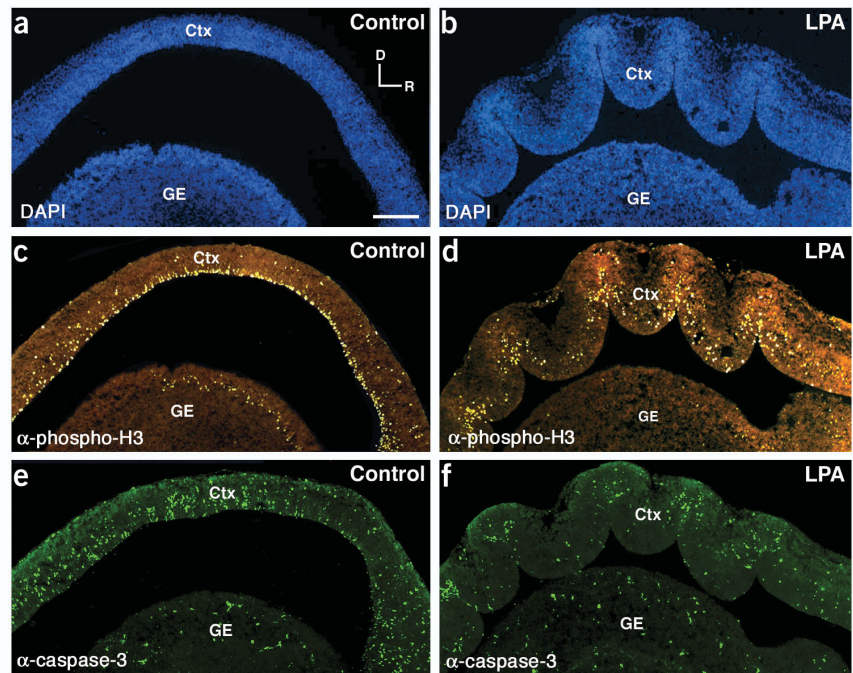


**Figure 6** LPA decreases cell death. (a,b) E14 cortices labeled with ISEL<sup>+</sup> (note pyknotic nuclei, black arrows) following culture with LPA (b) or control medium (a). CP, cortical plate; IZ, intermediate zone; SVZ, subventricular zone; VZ, ventricular zone. (c) Percentage of ISEL<sup>+</sup>-labeled pyknotic nuclei in control and LPA-treated cortices ( $n = 7$  matched pairs,  $*P = 0.04$ , paired  $t$ -test). Only pyknotic nuclei were counted (see Methods). (d,e) DAPI-stained E14 cortices immunolabeled for anti-active caspase-3 (green) following culture with LPA (e) or control medium (d). (f) Percentage of active caspase-3-labeled cells in control and LPA-treated cortices ( $n = 8$  matched pairs,  $*P = 0.02$ , paired  $t$ -test). Scale bars (a,b,d,e) represent 50  $\mu$ m.

**Figure 7** LPA's effects are observed throughout the telencephalon. (a,b) DAPI-stained E14 cortices showing increased cortical thickness throughout the rostral-caudal dimensions of cortex following culture with LPA (b) compared with control medium (a). (c,d) E14 cortices immunolabeled for anti-phospho-H3 (red) showing displacement of mitotic cells throughout the rostral-caudal dimensions of cortex following culture with LPA (d) compared with control medium (c). (e,f) E14 cortices immunolabeled for antibody to active caspase-3 (green) showing decreased cell death throughout the rostral-caudal dimensions of cortex following culture with LPA (f) compared with control medium (e). D, dorsal; R, rostral; Ctx, cortex; GE, ganglionic eminence. Scale bar, 200  $\mu$ m.



ated LPA signaling increased cortical thickness by altering both proliferative and postmitotic populations, and it further produced regularly arranged cortical folds. We infer from our data that specific cortical changes observed after LPA treatment were due to (i) the increased survival of many NPCs, which enlarged the proliferating pool and (ii) the induction of terminal mitosis in NPCs, which increased the number of postmitotic neurons. It is worth noting that the increased presence of  $\beta$ -tubulin-III-labeled cells in the VZ following LPA treatment may represent premature differentiation of NPCs that contribute to increased VZ thickness. Our results are not likely explained by altered cell cycle parameters, as S/G<sub>2</sub>-M transition times *ex vivo* were indistinguishable from those reported *in vivo*<sup>24</sup>, and LPA treatment did not increase the number of S-phase cells, consistent with the completion of approximately one full cell cycle during the 17-h *ex vivo* culture. A hypothetical increase in migration velocity in the presence of LPA can not explain our results, as (i) migration in the absence of increased cell production can not increase cortical size, and (ii) the number of BrdU-labeled cells reaching postmitotic regions was indistinguishable between LPA-treated and untreated cortices after a short interval (Fig. 5g).

LPA is known to activate multiple pathways that produce a range of biological responses, including proliferation, survival, gap-junction closure, Ca<sup>2+</sup> mobilization, membrane depolarization and cytoskeletal remodeling in many cell types<sup>11,27,35</sup>. In the VZ, cytoskeletal changes have been proposed to trigger the 'rounding up phase' of NPCs during interkinetic nuclear migration<sup>17</sup>, consistent with the increased number of mitotic profiles described here for LPA-treated cortices. Importantly, cytoskeletal changes occur in minutes following LPA exposure<sup>14,36,37</sup>, which stands in contrast to the 6-h latency between LPA exposure and visible cortical folds. This temporal disparity indicates that additional LPA-mediated pathways beyond those mediating the rapid cytoskeletal changes are required to produce the observed folding. The time course for increasing cortical thickness and cell number and the involved LPA-mediated pathways remain to be determined.

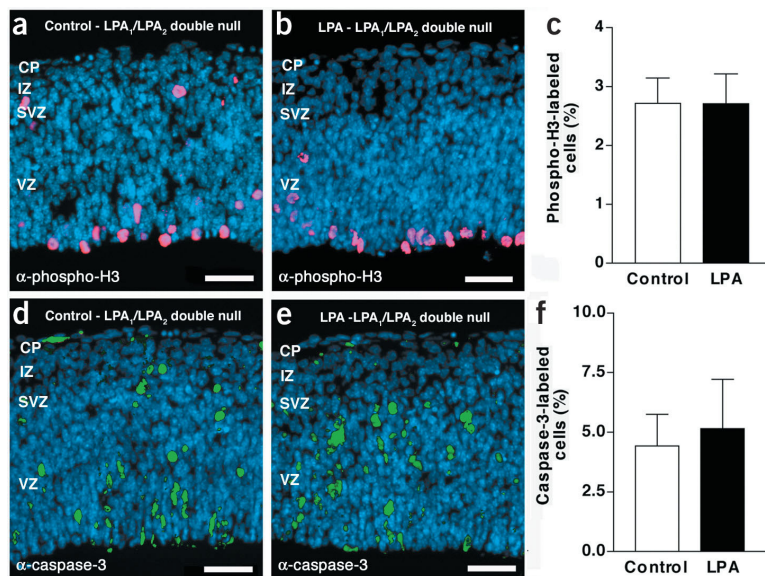


**Figure 8** Effects of LPA are absent in mice null for both LPA<sub>1</sub> and LPA<sub>2</sub>. (a,b) DAPI-stained E14 cortices from a LPA<sub>1</sub> LPA<sub>2</sub> double-null mouse cultured with control medium (a) or 1  $\mu$ M LPA (b), immunolabeled for anti-phospho-H3 (red). CP, cortical plate; IZ, intermediate zone; SVZ, subventricular zone; VZ, ventricular zone. (c) Percentage of phospho-H3-labeled cells in control and LPA-treated cortices from LPA<sub>1</sub> LPA<sub>2</sub> double-null mice ( $n = 4$  matched pairs,  $P = 0.97$ , paired  $t$ -test). (d,e) DAPI-stained E14 cortices from a LPA<sub>1</sub> LPA<sub>2</sub> double-null mouse cultured with control medium (d) or 1  $\mu$ M LPA (e), immunolabeled for antibody to active caspase-3 (green). (f) Percentage of active caspase-3-labeled cells in control and LPA-treated cortices from LPA<sub>1</sub> LPA<sub>2</sub> double-null mice ( $n = 4$  matched pairs,  $P = 0.4$ , paired  $t$ -test). Scale bars in a,b,d,e, 50  $\mu$ m.

The observation that postmitotic neurons in culture release tenfold more LPA than NPCs suggests the operation of a feedback mechanism influencing neuroblasts<sup>17</sup>. This form of feedback may modulate NPC survival and terminal mitosis, as reported here. Mechanisms of LPA production in the cortex are unknown, but could involve autotaxin, recently reported as a lysophospholipase-D enzyme that can produce LPA<sup>38,39</sup>. Moreover, PRG-1, a new lipid phosphate phosphatase that can degrade LPA, could also control LPA-signaling by reducing the local concentration of active phospholipids within the central nervous system<sup>40</sup>.

Several corollaries relevant to cortical growth and the effects of LPA extend from our data. First, the present results indicate that growth can occur very rapidly—within 17 h—compared with the days of growth required to observe FGF2-dependent NPC proliferation<sup>7,9</sup>. This rapid increase after LPA exposure is consistent with studies showing that rescue of NPC death—likely multiple rounds of death given the ~2 h clearance time estimated for dying cells in the cortex<sup>41</sup>—can have major consequences for cortical growth<sup>4,33</sup>. Second, the displacement of mitotic cells following LPA treatment suggests that neurogenesis and interkinetic nuclear migration can be uncoupled while still allowing the formation of a stratified cerebral wall. Third, our results indicate that the cortex need not be constrained by structures such as the skull to undergo folding, as previously suggested<sup>42</sup>, and are consistent with theories that emphasize intracortical mechanisms in the generation of folds<sup>43,44</sup>. Fourth, genetic modifications of LPA signaling pathways may have influenced the expansion of cerebral cortical size across mammalian evolution since LPA regulates two neurogenic processes known to affect cortical growth and thickness. Fifth, the unexpected finding that LPA did not increase NPC proliferation indicates that lipid effects within organized tissues may be distinct from those observed in dissociated cell culture<sup>18</sup>. Finally, LPA's effects on NPCs observed here could have therapeutic relevance for both neural stem cell maintenance<sup>45,46</sup> and medicinal approaches, in view of data supporting lysophospholipid receptors as viable drug targets in humans<sup>47</sup>.

In summary, our results implicate small lipid signals acting through cognate receptors as new influences on cerebral cortical growth and anatomy. The existence of related lipid signals and receptors expressed within the neuraxis<sup>11</sup> suggests an expanding range of lipid influences for the developing and mature nervous system.

## METHODS

**Cortical hemisphere cultures.** Animal protocols were approved by the Animal Subjects Committee at the University of California at San Diego and the Animal Research Committee at The Scripps Research Institute, and conformed to National Institutes of Health guidelines and public law. Timed-pregnant BALB/c females (Simonsen Laboratories), C57Bl/6 females or LPA<sub>1</sub> LPA<sub>2</sub> double-heterozygous females (on a mixed background (C57Bl/6 × 129SW) were killed by halothane followed by cervical dislocation, and embryos were removed at E14. Embryos from the LPA<sub>1</sub> LPA<sub>2</sub> double-heterozygous females were genotyped by PCR using DNA isolated from a small part of the tail<sup>18,19</sup>. Brains of embryos were dissected in serum-free medium: Opti-MEM I (Gibco/BRL) containing 20 mM D-glucose, 55 μM β-mercaptoethanol and 1% penicillin-streptomycin. The two cortical hemispheres of each brain were separated along the midline. One hemisphere was cultured in medium containing 1 μM LPA (Oleoyl-LPA, Avanti Polar Lipids) in 0.1% fatty-acid free bovine serum albumin (FAFBSA; Sigma), the other in control medium containing 0.1% FAFBSA. A concentration of 1 μM LPA was chosen because this concentration approximates maximum receptor occupancy in culture<sup>14,48</sup> and has been shown to be effective in inducing NPC cytoskeletal changes within explants<sup>17</sup>. Hemispheres were cultured at 37 °C for 16–18 h, shaking at 65 r.p.m. At the end of culture, matched hemispheres were fixed in 4% paraformaldehyde (PFA) in 0.1 M phosphate buffered saline (pH 7.4), cry-

protected in graded sucrose solutions to 30%, embedded in Tissue-Tek (Sakura) and rapidly frozen on dry ice. Tissue was cut sagittally at 10 μm on a cryostat and mounted onto Superfrost Plus slides (Fisher Scientific).

**Time course analysis.** Hemisphere cultures were prepared as described above. In a few cases, time *ex vivo* was extended to 24 h. To track cortical folding, digital photos of hemispheres treated with LPA were taken at 0 h, 1 h, 2 h, 3 h, 4 h, 6 h, 8 h, 10 h, 12 h, 14 h, 16 h and 24 h using a Nikon COOLPIX 950 digital camera. Photos of paired control hemispheres were taken at 0 h and 16 h. Between six and ten paired hemispheres were examined at each time point. Living cultures and digital photos were analyzed for cortical folding for each hemisphere. Cortical folding was identified by distortions of the cortical surface.

**BrdU labeling.** For most experiments, BrdU (Boehringer Mannheim) was diluted in sterile dH<sub>2</sub>O and added to cultures at a concentration of 40 μM. To determine the location of S-phase cells, explants were exposed to BrdU 1 h before the end of culture. To examine interkinetic nuclear migration, explants were exposed to BrdU 5 h before the end of culture. To assess cell migration into the cortical plate, E14 timed-pregnant BALB/c mice were injected intraperitoneally with 20 μl per g body weight of 10 mM BrdU in sterile saline and killed 1 h after injection. The brains of embryos were then prepared for 17 h as cortical explant cultures. To examine cell cycle progression, S-phase cells labeled by a 1-h BrdU pulse were examined at subsequent time points for entry and exit from M-phase. Specifically, matched hemispheres cultured with or without LPA for 10 h received a 1-h BrdU pulse. After the pulse, media containing BrdU was replaced with previous LPA or control media, and matched cortices were cultured for an additional 1, 3, 5 or 7 h. To determine how many BrdU-labeled cells were in mitosis at each time point, we counted the number of cells co-stained with antibody specific to BrdU (anti-BrdU) and anti-phospho-H3. To compare neuronal cell migration out of the VZ in control and LPA conditions, matched hemispheres cultured with or without LPA for 10 h received a 1-h BrdU pulse. After the pulse, cortices were cultured for an additional 7 h, and the number of BrdU-labeled cells in postmitotic zones was examined as previously described *in vivo*<sup>49</sup>.

**DNA synthesis measurements.** [<sup>3</sup>H]thymidine experiments were done as previously described<sup>50</sup>. Briefly, [<sup>3</sup>H]thymidine (NEN Life Science Products) was added to control and LPA medium at a concentration of 1 μCi/ml and cerebral hemisphere explants were cultured for 17 h. Explants were washed twice with serum-free medium, incubated overnight with 0.4 M NaOH and homogenized. Aliquots of the homogenates were precipitated with 50 μl of the NaOH solution added to 5 ml of cold 10% trichloro-acetic acid (TCA; Sigma) and collected on GF/A Whatman filters (Fisher Scientific). After an additional wash with 10% TCA and three washes with 100% ethanol, filters were dried at 80 °C for 30 min. Once dry, filters were placed in 10 ml Ecolume (ICN) for scintillation counts in a Beckman LS 1701 scintillation analyzer. [<sup>3</sup>H]thymidine counts were obtained from 12 matched cerebral hemispheres from three independent experiments.

**Immunohistochemistry and ISEL<sup>+</sup>.** Monoclonal antibodies used for staining NPCs and postmitotic neurons were anti-BrdU (Boehringer Mannheim), anti-*nestin* (PharMingen) and anti-β-tubulin III (Chemicon). Rabbit polyclonals used were anti-phospho-H3 (Upstate Biotechnology) and antibody specific to cleaved caspase-3 (Cell Signaling). Primary antibodies were detected with Cy3- or FITC-conjugated goat anti-mouse or Cy3-conjugated donkey anti-rabbit antibodies (Jackson Immunoresearch). Tissue was processed according to standard protocols. BrdU immunolabeling was performed according to former protocols<sup>4</sup> and visualized with FITC-conjugated goat anti-mouse or 3,3'-diaminobenzidine tetrahydrochloride (Sigma) as the chromogen. To identify pyknotic cells, tissue underwent ISEL<sup>+</sup> processing as previously described<sup>30</sup>, with the modification that cortices were fixed in 4% PFA before sectioning, rather than fresh frozen, to preserve histology. Because this procedural modification results in reduced sensitivity, we focused on ISEL<sup>+</sup>-labeled pyknotic nuclei since these cells are the most robustly labeled. Tissue sections in the various experiments were counterstained with the nuclear stain, 4',6'-diamino-2-phenylindole (DAPI; Sigma) or with the Nissl stain, cresyl violet. Proliferative and postmitotic cortical zones were delin-

eated by immunolabeling the same or adjacent sections with anti-Ki67 (Pharmingen) or anti-proliferating cell nuclear antigen (Oncogene) and anti- $\beta$ -tubulin III or antibody to microtubule associated protein 2 (Sigma), respectively. Images were prepared using Adobe Photoshop 7.0 and Adobe Illustrator 10 (Adobe Systems).

**Quantification of labeled cells.** All experimenters were blind to the conditions during counting. In medial cortex, sagittal cross-sections (~200  $\mu$ m across by width of cortex from pial to ventricular surface) from anterior, middle and/or posterior cortex, matched for location in control and LPA-treated hemispheres, were captured with an AxioCam digital camera (Zeiss). Labeled cells were scored in Adobe Photoshop 5.0 and quantified in NIH Image 1.62 software. In most instances, cell counts were expressed as a percentage of total cell number per cross-section, determined by counting counterstained DAPI nuclei. For analyses of cell cycle parameters, the number of cells double-labeled with anti-BrdU and anti-phospho-H3 was expressed as a percentage of the total number of phospho-H3-labeled cells. For counts of BrdU-labeled cells in postmitotic regions, matched cross-sections from anterior, middle and/or posterior cortex (350  $\mu$ m across by width of cortex from pial to ventricular surface) were used. The border between proliferative and postmitotic regions was defined by immunolabeling with anti-Ki-67. Cell counts for the six different analyses were obtained from 2–5 independent experiments. Comparisons between control and experimental groups were made using paired *t*-tests in Statview 5.0 (SAS Institute Inc.).

**Quantification of cell density and cell size.** All experimenters were blind to the conditions during counting. To determine cell density, a 30  $\times$  100  $\mu$ m rectangle was placed randomly in the VZ and IZ/CP of 12 matched cross-sections from seven pairs of control and LPA-treated cortices. The number of cells (981 and 971 total cells in VZ and IZ/CP, respectively) falling within the rectangle was counted for the two cortical zones.

To determine cell size, a cell's length and width (*x* and *y* axes) were measured and an average cell diameter was computed for each cell from nestin-immunolabeled profiles. Approximately 30 cells per cross-section (184 total cells) were analyzed at randomly selected locations throughout the VZ from three control and LPA-treated hemispheres. Cell density and cell size comparisons between control and experimental groups were made using paired *t*-tests in Statview 5.0.

#### ACKNOWLEDGMENTS

The authors thank B. Friedman, D. Kaushal, M. McConnell, A. Yang, X. Ye and J. H. Brown for useful discussions regarding this work; B. Almeida, M. Fontanoz, J. Goodson and G. Kennedy for technical assistance; J. Goodson for critical reading of this manuscript; and H. Karten for assistance with photography. This work was supported by the National Institute of Mental Health and Human Frontiers Science Program (J.C.), a Neuroplasticity of Aging Training Grant postdoctoral fellowship from the National Institute of Aging (M.A.K.), a postdoctoral fellowship from the PEW Latin American Fellows in the Biomedical Sciences (S.K.R.), a predoctoral fellowship from the Howard Hughes Medical Institute and a Merck fellow award (C.M.H.) and The Helen I. Dorris Institute for the Study of Neurological and Psychiatric Disorders of Children and Adolescents (J.C., M.A.K., S.K.R., C.M.H.).

#### COMPETING INTERESTS STATEMENT

The authors declare that they have no competing financial interests.

Received 1 August; accepted 16 October 2003

Published online at <http://www.nature.com/natureneuroscience/>

- Rakic, P. A small step for the cell, a giant leap for mankind: a hypothesis of neocortical expansion during evolution. *Trends Neurosci.* **18**, 383–388 (1995).
- Caviness, V.S.Jr., Takahashi, T. & Nowakowski, R.S. Numbers, time and neocortical neurogenesis: a general developmental and evolutionary model. *Trends Neurosci.* **18**, 379–383 (1995).
- Haydar, T.F., Kuan, C.Y., Flavell, R.A. & Rakic, P. The role of cell death in regulating the size and shape of the mammalian forebrain. *Cereb. Cortex* **9**, 621–626 (1999).
- Pompeiano, M., Blaschke, A.J., Flavell, R.A., Srinivasan, A. & Chun, J. Decreased apoptosis in proliferative and postmitotic regions of the caspase 3-deficient embryonic central nervous system. *J. Comp. Neurol.* **423**, 1–12 (2000).
- LoTurco, J.J., Owens, D.F., Heath, M.J., Davis, M.B. & Kriegstein, A.R. GABA and glutamate depolarize cortical progenitor cells and inhibit DNA synthesis. *Neuron* **15**, 1287–1298 (1995).

- Drago, J., Murphy, M., Carroll, S.M., Harvey, R.P. & Bartlett, P.F. Fibroblast growth factor-mediated proliferation of central nervous system precursors depends on endogenous production of insulin-like growth factor I. *Proc. Natl. Acad. Sci. USA* **88**, 2199–2203 (1991).
- Ghosh, A. & Greenberg, M.E. Distinct roles for bFGF and NT-3 in the regulation of cortical neurogenesis. *Neuron* **15**, 89–103 (1995).
- Temple, S. & Qian, X. bFGF, neurotrophins and the control of cortical neurogenesis. *Neuron* **15**, 249–252 (1995).
- Vaccaro, F.M. *et al.* Changes in cerebral cortex size are governed by fibroblast growth factor during embryogenesis. *Nat. Neurosci.* **2**, 246–253 (1999).
- Suh, J., Lu, N., Nicot, A., Tatsuno, I. & DiCicco-Bloom, E. PACAP is an anti-mitogenic signal in developing cerebral cortex. *Nat. Neurosci.* **4**, 123–124 (2001).
- Fukushima, N., Ishii, I., Contos, J.J., Weiner, J.A. & Chun, J. Lysophospholipid receptors. *Annu. Rev. Pharmacol. Toxicol.* **41**, 507–534 (2001).
- Chun, J. *et al.* International union of pharmacology. XXXIV. Lysophospholipid receptor nomenclature. *Pharmacol. Rev.* **54**, 265–269 (2002).
- Contos, J.J. & Chun, J. The mouse *lpa<sub>3</sub>/Edg7* lysophosphatidic acid receptor gene: genomic structure, chromosomal localization, and expression pattern. *Gene* **267**, 243–253 (2001).
- Hecht, J.H., Weiner, J.A., Post, S.R. & Chun, J. Ventricular zone gene-1 (*vzq-1*) encodes a lysophosphatidic acid receptor expressed in neurogenic regions of the developing cerebral cortex. *J. Cell. Biol.* **135**, 1071–1083 (1996).
- McGiffert, C., Contos, J.J., Friedman, B. & Chun, J. Embryonic brain expression analysis of lysophospholipid receptor genes suggests roles for *s1p<sub>1</sub>* in neurogenesis and *s1p<sub>1-3</sub>* in angiogenesis. *FEBS Lett.* **531**, 103–108 (2002).
- Dubin, A.E., Bahnsen, T., Weiner, J.A., Fukushima, N. & Chun, J. Lysophosphatidic acid stimulates neurotransmitter-like conductance changes that precede GABA and L-glutamate in early, presumptive cortical neuroblasts. *J. Neurosci.* **19**, 1371–1381 (1999).
- Fukushima, N., Weiner, J.A. & Chun, J. Lysophosphatidic acid (LPA) is a novel extracellular regulator of cortical neuroblast morphology. *Dev. Biol.* **228**, 6–18 (2000).
- Contos, J.J., Fukushima, N., Weiner, J.A., Kaushal, D. & Chun, J. Requirement for the *lpa<sub>1</sub>* lysophosphatidic acid receptor gene in normal suckling behavior. *Proc. Natl. Acad. Sci. USA* **97**, 13384–13389 (2000).
- Contos, J.J. *et al.* Characterization of *lpa<sub>2</sub>* (*Edg4*) and *lpa<sub>1</sub>/lpa<sub>2</sub>* (*Edg2/Edg4*) lysophosphatidic acid receptor knockout mice: signaling deficits without obvious phenotypic abnormality attributable to *lpa<sub>2</sub>*. *Mol. Cell Biol.* **22**, 6921–6929 (2002).
- Sauer, F. Mitosis in the neural tube. *J. Comp. Neurol.* **62**, 377–405 (1935).
- Sidman, R.L., Miale, I.L. & Feder, N. Cell proliferation and migration in the primitive ependymal zone: an autoradiographic study of histogenesis in the nervous system. *Exp. Neurol.* **1**, 322–333 (1959).
- Hendzel, M.J. *et al.* Mitosis-specific phosphorylation of histone H3 initiates primarily within pericentromeric heterochromatin during G2 and spreads in an ordered fashion coincident with mitotic chromosome condensation. *Chromosoma* **106**, 348–360 (1997).
- Rehen, S.K. *et al.* Chromosomal variation in neurons of the developing and adult mammalian nervous system. *Proc. Natl. Acad. Sci. USA* **98**, 13361–13366 (2001).
- Takahashi, T., Nowakowski, R.S. & Caviness, V.S.Jr. Cell cycle parameters and patterns of nuclear movement in the neocortical proliferative zone of the fetal mouse. *J. Neurosci.* **13**, 820–833 (1993).
- Takahashi, T., Nowakowski, R.S. & Caviness, V.S., Jr. The cell cycle of the pseudostriated ventricular epithelium of the embryonic murine cerebral wall. *J. Neurosci.* **15**, 6046–6057 (1995).
- Cai, L., Hayes, N.L. & Nowakowski, R.S. Local homogeneity of cell cycle length in developing mouse cortex. *J. Neurosci.* **17**, 2079–2087 (1997).
- Moolenaar, W.H. Lysophosphatidic acid signalling. *Curr. Opin. Cell Biol.* **7**, 203–210 (1995).
- Menezes, J.R. & Luskin, M.B. Expression of neuron-specific tubulin defines a novel population in the proliferative layers of the developing telencephalon. *J. Neurosci.* **14**, 5399–5416 (1994).
- Ye, X., Ishii, I., Kingsbury, M.A. & Chun, J. Lysophosphatidic acid as a novel cell survival/apoptotic factor. *Biochim. Biophys. Acta.* **1585**, 108–113 (2002).
- Blaschke, A.J., Staley, K. & Chun, J. Widespread programmed cell death in proliferative and postmitotic regions of the fetal cerebral cortex. *Development* **122**, 1165–1174 (1996).
- Blaschke, A.J., Weiner, J.A. & Chun, J. Programmed cell death is a universal feature of embryonic and postnatal neuroproliferative regions throughout the central nervous system. *J. Comp. Neurol.* **396**, 39–50 (1998).
- Ishii, I., Contos, J.J., Fukushima, N. & Chun, J. Functional comparisons of the lysophosphatidic acid receptors, *LP<sub>A1</sub>/VZG-1/EDG-2*, *LP<sub>A2</sub>/EDG-4*, and *LP<sub>A3</sub>/EDG-7* in neuronal cell lines using a retrovirus expression system. *Mol. Pharmacol.* **58**, 895–902 (2000).
- Kuida, K. *et al.* Decreased apoptosis in the brain and premature lethality in CPP32-deficient mice. *Nature* **384**, 368–372 (1996).
- Chenn, A. & Walsh, C.A. Regulation of cerebral cortical size by control of cell cycle exit in neural precursors. *Science* **297**, 365–369 (2002).
- Ishii, I., Fukushima, N., Ye, X. & Chun, J. Lysophospholipid receptors: signaling and biology. *Annu. Rev. Biochem.* (in press).
- Fukushima, N. *et al.* Lysophosphatidic acid influences the morphology and motility of young, postmitotic cortical neurons. *Mol. Cell Neurosci.* **20**, 271–282 (2002).
- Jalink, K., Eichholtz, T., Postma, F.R., van Corven, E.J. & Moolenaar, W.H. Lysophosphatidic acid induces neuronal shape changes via a novel, receptor-mediated signaling pathway: similarity to thrombin action. *Cell Growth Differ.* **4**, 247–255 (1993).

38. Umez-Goto, M. *et al.* Autotaxin has lysophospholipase D activity leading to tumor cell growth and motility by lysophosphatidic acid production. *J. Cell. Biol.* **158**, 227–233 (2002).
39. Tokumura, A. *et al.* Identification of human plasma lysophospholipase D, a lysophosphatidic acid-producing enzyme, as autotaxin, a multifunctional phosphodiesterase. *J. Biol. Chem.* **277**, 39436–39442 (2002).
40. Brauer, A.U. *et al.* A new phospholipid phosphatase, PRG-1, is involved in axon growth and regenerative sprouting. *Nat. Neurosci.* **6**, 572–578 (2003).
41. Thomaïdou, D., Mione, M.C., Cavanagh, J.F. & Parnavelas, J.G. Apoptosis and its relation to the cell cycle in the developing cerebral cortex. *J. Neurosci.* **17**, 1075–1085 (1997).
42. Le Gros Clark, W.E. Deformation patterns on the cerebral cortex. in *Essays on Growth and Form* (eds. Le Gros Clark, W.E. & Medawar, P.B.) 1–22 (Oxford Univ. Press, London, 1945).
43. Richman, D.P., Stewart, R.M., Hutchinson, J.W. & Caviness, V.S.Jr. Mechanical model of brain convolitional development. *Science* **189**, 18–21 (1975).
44. Barron, D.H. An experimental analysis of some factors involved in the development of fissure pattern of the cerebral cortex. *J. Exp. Zool.* **113**, 553–573 (1950).
45. Gage, F.H. Mammalian neural stem cells. *Science* **287**, 1433–1438 (2000).
46. Alvarez-Buylla, A., Garcia-Verdugo, J.M. & Tramontin, A.D. A unified hypothesis on the lineage of neural stem cells. *Nat. Rev. Neurosci.* **2**, 287–293 (2001).
47. Mandala, S. *et al.* Alteration of lymphocyte trafficking by sphingosine-1-phosphate receptor agonists. *Science* **296**, 346–349 (2002).
48. Fukushima, N., Kimura, Y. & Chun, J. A single receptor encoded by *vzq-1/IpA1/edg-2* couples to G proteins and mediates multiple cellular responses to lysophosphatidic acid. *Proc. Natl. Acad. Sci. USA* **95**, 6151–6156 (1998).
49. Takahashi, T., Nowakowski, R.S. & Caviness, V.S., Jr. Interkinetic and migratory behavior of a cohort of neocortical neurons arising in the early embryonic murine cerebral wall. *J. Neurosci.* **16**, 5762–5776 (1996).
50. Rehen, S.K., Cid, M., Fragel-Madeira, L. & Linden, R. Differential effects of cyclin-dependent kinase blockers upon cell death in the developing retina. *Brain Res.* **947**, 78–83 (2002).